frontiers in Earth Science

ORIGINAL RESEARCH
published: 01 November 2021
doi: 10.3389/feart.2021.788738

Rapid Northwestward Extension of the East Asian Summer Monsoon Since the Last Deglaciation: Evidence From the Mollusk Record

Yajie Dong[1]*, Naiqin Wu[1]*, Fengjiang Li[1,2,3] and Houyuan Lu[1,4]

[1]Key Laboratory of Cenozoic Geology and Environment, Institute of Geology and Geophysics, Chinese Academy of Sciences, Beijing, China, [2]Innovation Academy for Earth Science, Chinese Academy of Sciences, Beijing, China, [3]Center for Excellence in Life and Paleoenvironment, Chinese Academy of Sciences, Beijing, China, [4]College of Earth and Planetary Sciences, University of Chinese Academy of Sciences, Beijing, China

The magnitude and rate of the expansion of the East Asian summer monsoon (EASM) rain belt under future climatic warming are unclear. Appropriate ecological proxy data may provide an improved understanding of the spatial extension of the EASM during past warming intervals. We reconstructed the spatiotemporal pattern of the extension of the EASM since the Last Glacial Maximum (LGM), using six well-dated mollusk fossil sequences from Chinese loess sections located on the modern northern edge of the EASM. The abundance of typical dominant mollusk species indicative of EASM intensity shows a delayed response, from ~17 ka in the southeastern sections to ~9 ka in the northwestern sections, during the last deglacial warming. Isoline plots based on a mollusk data synthesis show that the mollusk EASM indicators have a northeast–southwest zonal distribution for both the present-day, the cold LGM, and the warm mid-Holocene, which is consistent with the spatial pattern of modern precipitation. The resulting estimated expansion rate of EASM intensity accelerated during ~12–9 ka (~50 km/ka), which corresponds to the early Holocene interval of rapid climatic warming, a northwestward shift of ~150 km compared to today. This implies that the northern fringe of the EASM in northern China will become wetter in the coming century, under moderate warming scenarios.

Keywords: last deglaciation, land snails, monsoon margin, climatic warming, loess plateau

OPEN ACCESS

Edited by:
Zhuolun Li,
Lanzhou University, China

Reviewed by:
Pál Sümegi,
University of Szeged, Hungary
Daniel Enrique Ibarra,
Brown University, United States

****Correspondence:***
Yajie Dong
dongyajie@mail.iggcas.ac.cn
Naiqin Wu
nqwu@mail.iggcas.ac.cn

Specialty section:
This article was submitted to Quaternary Science, Geomorphology and Paleoenvironment, a section of the journal Frontiers in Earth Science

Received: *03 October 2021*
Accepted: *19 October 2021*
Published: *01 November 2021*

Citation:
Dong Y, Wu N, Li F and Lu H (2021) Rapid Northwestward Extension of the East Asian Summer Monsoon Since the Last Deglaciation: Evidence From the Mollusk Record. Front. Earth Sci. 9:788738. doi: 10.3389/feart.2021.788738

INTRODUCTION

The East Asian summer monsoon (EASM) serves as an interhemispheric heat transfer mechanism and is the main mechanism of moisture transport to East Asia (Webster et al., 1998; Ding, 2004). In recent decades, the summer monsoon rain belt has retreated southward, increasing the incidence of droughts in northern China and flooding in southern China (Wang, 2001; Chase et al., 2003; Ding et al., 2008). Several researchers have linked these monsoon migrations to recent global warming (Li et al., 2010), and argue that as the world warms, dry regions will become drier and wet regions will become wetter (Held and Soden, 2006). However, this scenario, which is based on limited decadal-scale observational data, has made it difficult to establish a long-term linkage between monsoon rainfall and climatic warming and has been challenged by paleo-records of the monsoon (Yang and Ding, 2008; Yang et al., 2015; Huang et al., 2019; Cheng et al., 2020).

Current paleoclimate records reflecting the variability of EASM rainfall intensity come mainly from oxygen isotopic records from cave deposits (Wang Y. J. et al., 2001; Cheng et al., 2006; Cheng et al., 2009), and physical and geochemical proxies (e.g., magnetic susceptibility, $\delta^{13}C$ of organic matter) from loess deposits and lake sediments (Lu et al., 2007; Peterse et al., 2011; Lu et al., 2013; Chen et al., 2015; Goldsmith et al., 2017; Wen et al., 2017). These studies addressing the response of the EASM to past warming focus on two main aspects: 1) Reconstructing the history of EASM rainfall intensity and exploring its relationship with the external drivers of climate forcing. Based on well-documented speleothems oxygen isotopic records, the debate over whether the EASM reached its maximum intensity in the early Holocene (Wang Y. J. et al., 2001; Cheng et al., 2006; Cheng et al., 2009) or the mid-Holocene (Lu et al., 2013; Chen et al., 2015) still challenges our understanding of the response of EASM intensity to summer insolation and the associated temperature fluctuations. 2) Spatial characterization of the magnitude of shifts in the EASM rain belt during past warming intervals, especially on the sensitive northern fringe, which is of particular eco-environmental concern. Recent paleorecords based on the spatial distribution of C_4 plant biomass and loess grain size suggest that the EASM moved northwestward by ~300 km from the cold Last Glacial Maximum (LGM) to the warm mid-Holocene (~6 ka) (Yang and Ding, 2008; Yang et al., 2015). This northward shift in the EASM rainfall belt would have increased the precipitation in the semi-arid region of northern China, which is supported by PlioMIP climate simulations (Huang et al., 2019; Cheng et al., 2020).

Although these paleo-records and climate simulations indicate the same trend of northwestward migration of the northern extent of the EASM, the spatial estimates show only two time-slice scenarios (a warm mid-Holocene and a cold LGM). However, the rate and spatial extent of the movement of the EASM rain belt since the last deglaciation, and their relationship with warming rates, remain unclear. Since the validity of Chinese cave isotope-based reconstructions of EASM precipitation intensity has been questioned (Tan, 2009; Maher and Thompson, 2012; Liu et al., 2015), and other geological evidence is mainly from a few records from single sites, the extent to which the spatial migration of the EASM rain belt fluctuated under past climatic warming requires further investigation. Absent from the debate are multi-site records of ecological indicators sensitive to summer monsoon precipitation amount.

Terrestrial mollusks are one of the most diverse and abundant invertebrates inhabiting various environments of the East Asian monsoon regions (Nekola, 2003; Dong et al., 2019). They are abundantly preserved as fossils, for example in loess sediments (Rousseau and Wu, 1997; Wu et al., 2002; Sümegi et al., 2015; Horsák et al., 2018; Richter et al., 2019). Previous studies have shown that mollusks are sensitive to the advance and retreat of the East Asian monsoon, and several mollusks have been identified as indicator species of the EASM, such as *Punctum orphana* and *Macrochlamys angigyra* (Rousseau and Wu, 1997; Wu et al., 2002). These characteristics make mollusks a unique model taxon for exploring spatiotemporal changes in the EASM and their linkage with climatic warming.

Here we present the first modern distribution of terrestrial mollusks in northern China, together with six high-resolution mollusk fossil sequences spanning the interval from 25 ka (in the LGM) to the Holocene, along environmental gradients in the Chinese Loess Plateau (CLP), located in the northwestern part of the EASM region (**Figure 1**). The peripheral location of these loess sections with respect to the monsoon region provides an excellent opportunity to examine the magnitude of the spatial expansion of the EASM in response to climate change. The temperature of the Holocene climatic optimum (~8–4 ka) was ~2°C higher than today in the Northern Hemisphere (Wang S. et al., 2001; Shakun et al., 2012), which is equivalent to predicted warming. Our aims were to estimate the shift of the monsoon rain belt associated with past global warming and to predict future hydroclimatic trends in the region.

MATERIALS AND METHODS

Study Area and Sites

The six studied loess-palaeosol sections are Linxia (35°38′N, 103°09′E, H = 2,179 m), Huanxian (36°32′N, 107°20′E, H = 1,232 m), Shuozhou (39°23′N, 112°09′E, H = 1,579 m), Jingchuan (35°15′N, 107°43′E, H = 1,244 m), Jixian (36°06′N, 110°38′E, H = 995 m), and Yaoxian (34°53′N, 108°58′E, H = 673 m). They are located along a northwest–southeast transect across the CLP (**Figure 1A**). The northernmost sites (Linxia, Huanxian) are currently located near the northwestern limit of the EASM domain. The modern mean annual temperature (MAT) of these sites increases from ~6 to ~13°C, and the mean annual precipitation (MAP) from ~300 to ~650 mm, from northwest to southeast (**Figure 1A**). Daily backward moisture trajectories of rainfall events in the central CLP show that the moisture transported by the EASM accounts for ~85% of the annual rainfall (**Figure 1B**). About 70% of the precipitation falls in the summer and autumn seasons when the EASM circulation transports tropical and subtropical moisture inland (Qian, 1991).

Modern mollusk species distributions are from Li et al. (2016), Dong et al. (2019), Dong et al. (2020a). The dataset comprises 356 samples collected from surface soils across an ~800 km climatic gradient across northern China. This extensive dataset of modern mollusk samples covering all fossil sites ensures a comprehensive survey of species distributions.

Loess Sequences and Chronology

The six profiles are geographically located in "Yuan" areas (flat-topped loess highlands, covered with thick loess deposits), one of the major topographic units in the CLP (Liu, 1985). Sampling was undertaken on 1) the upper part of loess unit L1 (L1-1) which was deposited since marine isotope stage 2 (MIS2); and 2) the lower part of the Holocene paleosol

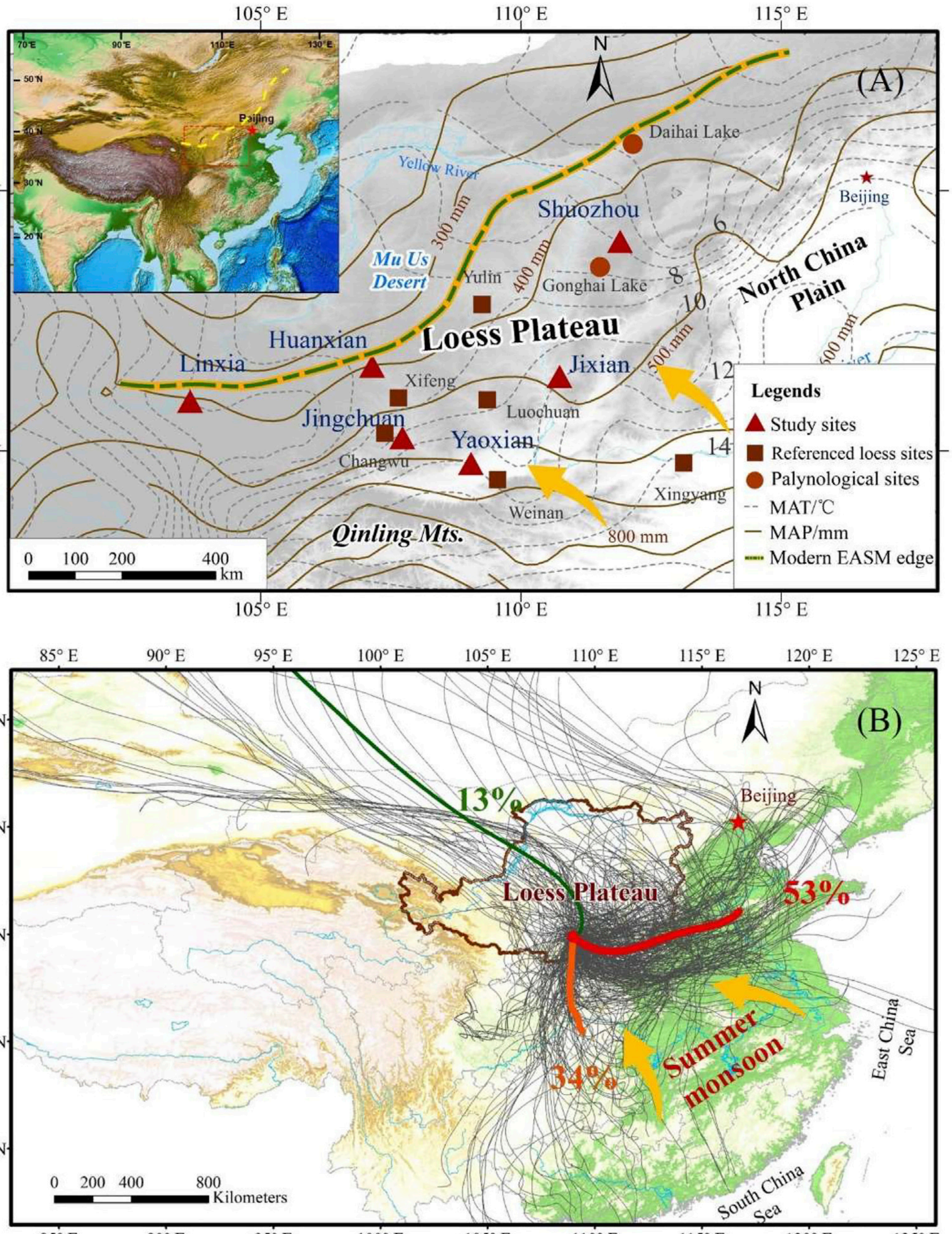

FIGURE 1 | Locations of the studied sections (solid red triangles) along climatic gradients from the northwest to southeast across the Chinese Loess Plateau **(A)**. The inset map shows the location of the study area and the modern northern edge of the EASM region. The arrows indicate the direction of the summer monsoonal winds. Brown squares and red circles denote locations of the loess sites and palynological sites referenced in the text. The isohyets (in mm; gray lines) and isotherms (in °C; brown dashed lines) are 50-years averages (Lin et al., 2002). **(B)** Ensembles of backward air-parcel trajectories (Draxler and Hess, 1997) of the source moisture for the Yaoxian loess site. Grey lines indicate daily backward (144 h) moisture trajectories of rainfall events (>0 mm/day) from January 2005 to December 2011, at the height of 1,000 m above ground level. Three primary moisture transport paths to the Yaoxian loess site were generated using cluster analysis of moisture trajectories. The green paths denote the Westerlies; the green paths denote the eastern branch of the East Asian summer monsoon; the red path denotes southern branches of the East Asian summer monsoon. The data for backward trajectories analysis were downloaded from (ftp://arlftp.arlhq.noaa.gov/pub/archives/reanalysis/).

unit (S0) (**Supplementary Figure S1**). The chronology of the six loess-paleosol sequences is based on high-resolution optically stimulated luminescence (OSL) dating for the Linxia, Huanxian, Jingchuan and Yaoxian sections (Lai and Wintle, 2006; Dong et al., 2015), and on the ^{14}C ages of mollusk shells from the Jixian (Dong et al., 2021a) and Shuozhou sections (**Supplementary Figure S2**). The age-depth models were constructed by polynomial fits through a number of successive absolute dates. The age-depth models for the loess sequence show that most of the loess profiles

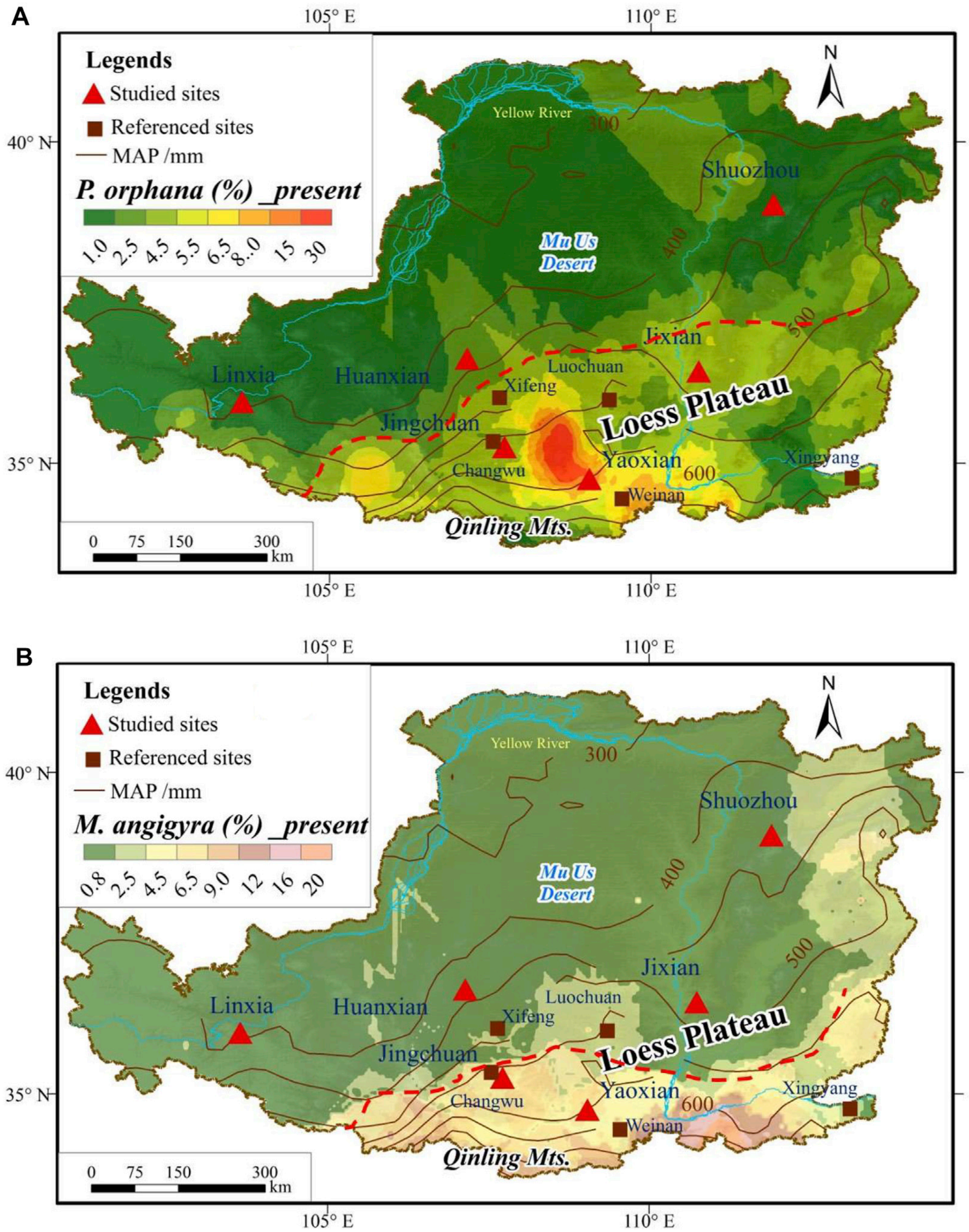

FIGURE 2 | Maps of the abundance of *P. orphana* **(A)** and *M. angigyra* **(B)** based on modern surveys (Li et al., 2016; Dong et al., 2019, 2020a), together with modern mean annual precipitation over the past 50 years. Red dotted lines show the reference values of the 4.5%, 2.5% isolines of *P. orphana* and *M. angigyra*, respectively.

span the past 25 ka, including the Last Glacial Maximum (LGM), the Last deglacial, and the Holocene (**Supplementary Figure S2**).

Mollusk Samples

A total of 522 mollusk samples were taken from the L1 and S0 strata in six loess sections spanning the last 22 ka. A sampling of each loess section was conducted at the equal intervals which equates to an average temporal resolution of ~200–600 years for each sample (**Supplementary Figure S1**). The mollusk data for the Yaoxian, Jingchuan, Linxia and Jixian loess profiles are from Dong et al. (2020a, 2020b, 2021b). Each sample comprised ~15 kg of soil material, and all samples were washed and sieved in the field using a 0.5-mm mesh sieve to remove fine soil. The mollusk shells were then picked and identified under a binocular microscope; the identification procedures followed Yen (1939) and Chen and Gao (1987). All mollusk taxa in the deposits were identified and the abundance of summer monsoon indicator species was determined at each site.

Spatial Analysis

Compared with the long geological period, the morphological and ecological characteristics of terrestrial mollusks, from the study area in northern China, have not changed since the LGM (Li et al., 2006), indicating that the range of potential evolutive variations remains very tight and negligible. This allows therefore to apply the present ecological requirements of the studied mollusk species to the Late glacial and Holocene malacofauna to assess the spatial dynamics of their distribution.

Interpolation analysis was used to produce a map of the spatial abundance of typical mollusk species for the whole study area. There are many spatial interpolation methods, such as Inverse Distance Weighted interpolation, Kriging interpolation algorithm and Natural Neighbor interpolation method (Sibson, 1981; Isaaks and Srivastava, 1989), used to predict the distribution of variables in different disciplines. Among them, Kriging interpolation, a geostatistical method, has been widely used to predict many environmental and ecological variables, such as annual rainfall and species richness, as long as the data are spatially dependent (Isaaks and Srivastava, 1989; Webster and Oliver, 2001). The Kriging interpolation involves a process of semi-variogram to model the spatial autocorrelation of the data to assign weights, which can result in better interpolations under an appropriate sampling design. In this study, this method was used for spatial analysis of the distribution of the mollusk species.

RESULTS

Mollusk Taxa Indicative of EASM Intensity

P. orphana and *M. angigyra* were two of the most abundant thermo-humidiphilous taxa, both in the modern mollusk samples and in the loess-paleosol sequences. Modern surveys based on the 356 surface mollusk samples (Li et al., 2016; Dong et al., 2019, 2020a) show that *P. orphana* has a mean abundance of ~5.3% in the CLP, with a maximum of ~46% (**Figure 2A**). The *P. orphana* isolines using the Kriging interpolation show a northeast–southwest trend (**Figure 2A**), which is consistent with the modern climatic pattern: i.e., a northeast–southwest trend (**Figure 1**). Its modern distribution is mainly in the southeastern CLP where the MAP ranges from ~450 to 860 mm, an area presently dominated by the summer monsoon.

M. angigyra, another typical thermo-humidiphilous species, requires a higher temperature and wetter conditions than *P. orphana* (Chen and Gao, 1987). Although its distribution is more southerly than that of *P. orphana*, they both show a similar spatial abundance pattern. From northwest to southeast, the abundance of *M. angigyra* increases substantially, reaching ~85%, and with an average of ~4.9% (**Figure 2B**). The abundance of these two mollusk species increases linearly with the increase in MAP in the CLP. Their spatial distribution shows that their abundance is sensitive to the hydrothermal regime in northern China and thus they reflect fluctuations in EASM intensity. Their occurrence on the northern fringe of EASM is regarded as a proxy of EASM strength and an indicator of the northward migration of the warm and wet summer monsoon into the Loess Plateau (Wu et al., 1996, 1999, 2002; Rousseau and Wu, 1997).

Spatial Patterns of Mollusk Abundance Since the LGM

Considering the sensitivity of the two mollusk species to the summer monsoon, and the fact that they are the dominant thermo-humidiphilous species in the entire mollusk assemblage, we now examine their spatiotemporal distribution since the LGM. The abundances of the two mollusk species show a striking and regular pattern of variability within the six loess sequences. In the southern region of the CLP (Yaoxian), *P. orphana* is abundant throughout the time series (**Figure 3A**). Large fluctuations in abundance occurred during 25–9 ka, but the species generally maintained a high level of abundance, with the average number of individuals remaining at ~30/15 kg (**Figure 3A**). The number of individuals of *P. orphana* was significantly reduced in the eastern and central CLP (Jixian, Jingchuan), and was almost absent before and during the LGM. The species began to be continuously distributed at ~20 ka at the Jixian site, and reached its maximum abundance during the early to middle Holocene. In the northern part of the CLP, the continuous presence of *P. orphana* in the Huanxian and Shuozhou sections was delayed by ~16 ka and 12.5 ka, respectively. In the far northwest Linxia section, the numbers of this species were even lower, and it did not appear until ~9 ka, although it increased substantially during the mid-Holocene (**Figure 3A**). At most of the sites *P. orphana* reached its maximum abundance between ~8 ka and ~4 ka, although there was a slight variability between the sites. Continuously declining abundances occurred during ~4–3 ka. In general, the sites in the northern CLP had a substantially lower abundance of *P. orphana* compared to the southern and eastern sites. During the last deglacial warming, the continuous occurrence of *P. orphana* was gradually delayed from southeast to northwest across the CLP.

The spatial abundance of *M. angigyra* is similar to that of *P. orphana*. Sites from the southern to the eastern CLP (Yaoxian, Jixian) contained more *M. angigyra* than most of the northern sites (Jingchuan, Huanxian, Shuozhou and Linxia) (**Figure 3B**). All of the sites had a low abundance of *M. angigyra* during the cold LGM. Between ~17 and 15 ka, there was a rapidly increasing abundance at sites in the eastern and southern CLP (Jixian, Yaoxian). Different from *P. orphana*, the northern boundary of the distribution of *M. angigyra* is much more southerly, being

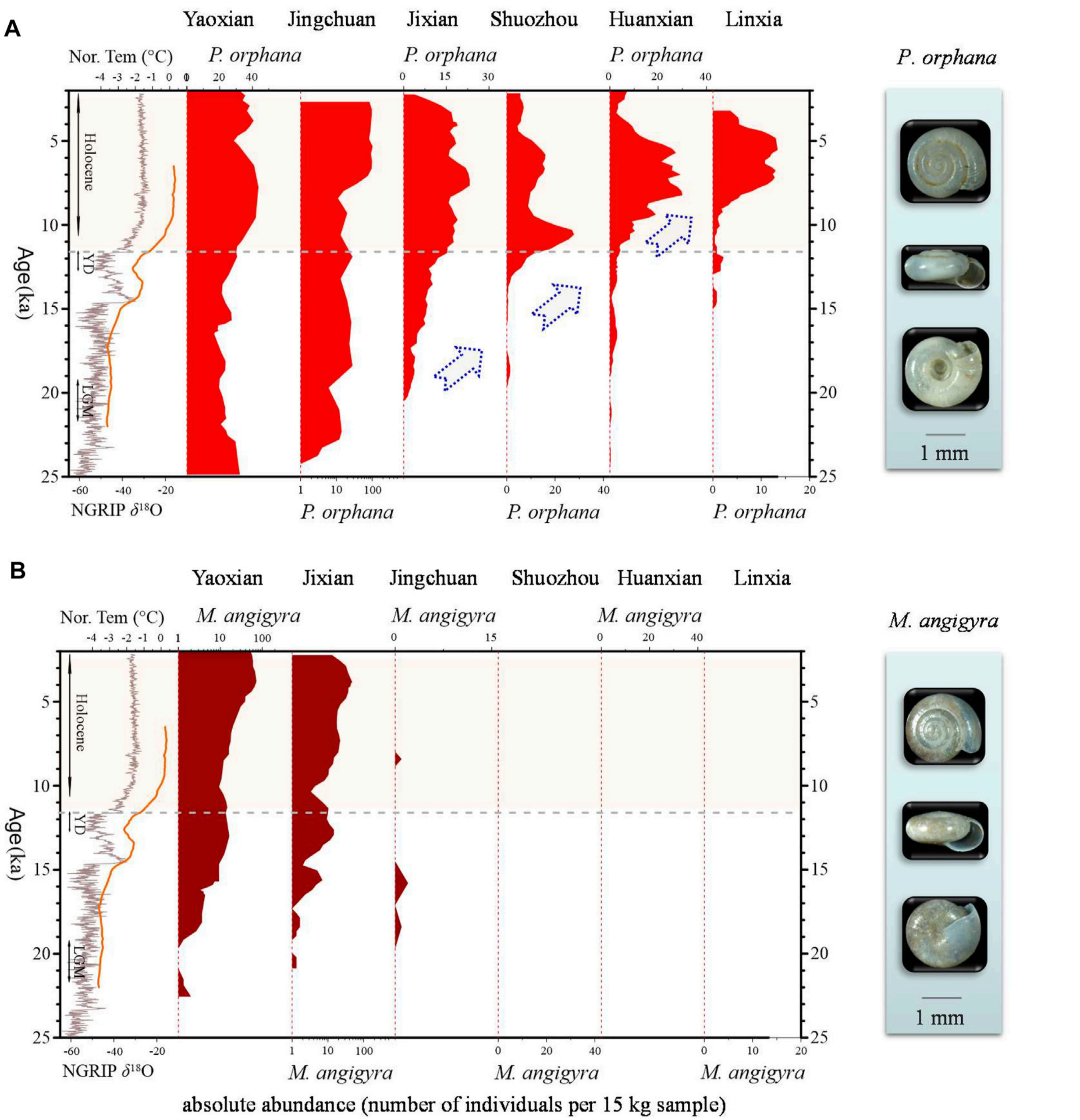

FIGURE 3 | Abundance of *P. orphana* **(A)** and *M. angigyra* **(B)** in the six loess sections from southeast to northwest across the Chinese Loess Plateau, and correlation with the Greenland NGRIP ice-core $\delta^{18}O$ record (Huber et al., 2006) and Northern Hemisphere average temperature (Nor. Tem) (°C) (Shakun et al., 2012). The Holocene, Younger Dryas (YD) and LGM intervals are indicated. The shaded zones indicate the Holocene soil layer.

rare or nearly absent from the central and northern areas, such as Jingchuan, Huanxian, Shuozhou and Linxia, during the entire Holocene.

Migration of the EASM Rain Belt From the LGM to the Middle Holocene

In order to characterize the spatial variation of the abundance of typical summer monsoon-sensitive mollusk species and to evaluate the extent of the summer monsoon, we plotted contour maps of their abundance based on a synthesis of the data from the present study and published fossil mollusk records (Wu et al., 1996, 1999, 2000, 2001, 2002, 2007; Rousseau and Wu, 1997; Rousseau et al., 2000, 2009). The isolines of the abundance of the two indicator mollusks all show a northeast–southwest zonal distribution during both the cold LGM, the warm Holocene, and at the present day (**Figure 4**). This pattern is consistent with the northeast–southwest trend of modern annual

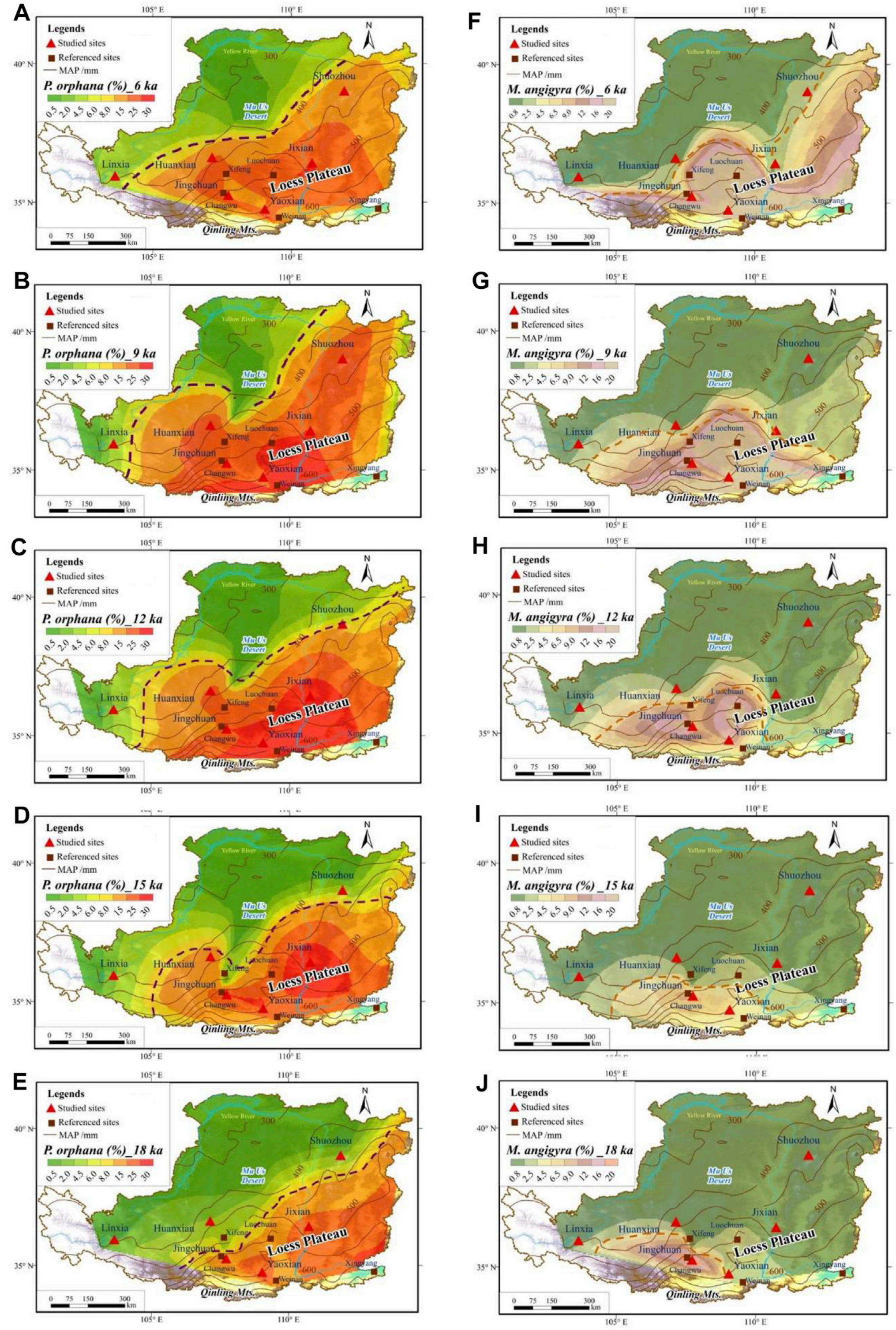

FIGURE 4 | Contour maps of the abundance of *P. orphana* and *M. angigyra* for the time slices of ~6 ka **(A, F)**, ~ 9 ka **(B, G)**, ~12 ka **(C, H)**, ~15 ka **(D, I)**, and ~18 ka **(E, J)** since the last deglaciation. The modern mean annual precipitation distribution over the past 50 years is also shown. Red dotted lines show the reference values of the 4.5 and 2.5% isolines of *P. orphana* and *M. angigyra*, respectively.

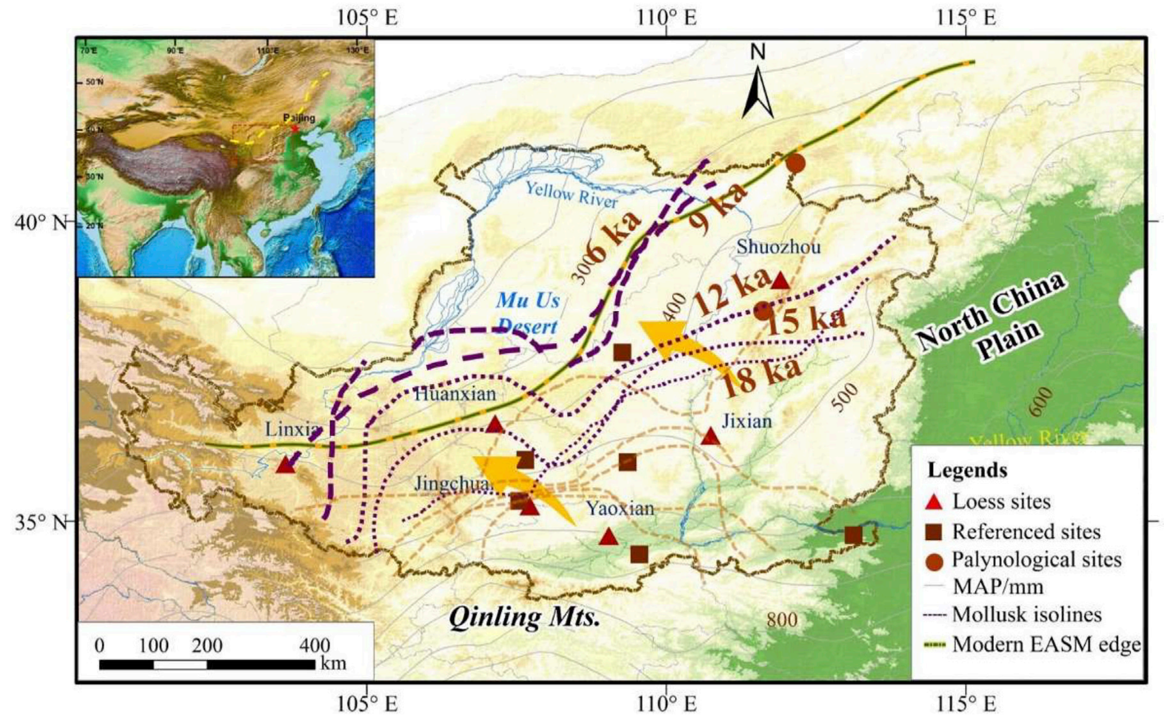

FIGURE 5 | Migration of the East Asian summer monsoon rain belt since the last deglaciation (~18 ka, ~15 ka, ~12 ka, ~9 ka, and ~6 ka) reconstructed using the abundance isolines for *P. orphana* (purple dotted line) and *M. angigyra* (orange dotted line).

isohyets. Therefore, changes in the zonal distribution of indicator mollusk abundance in the CLP can serve as a useful analog for shifts in the EASM rain belt. Since the 4.5% isoline of *P. orphana* abundance is close to the current northern limit of the EASM, we can use it as a reference value to estimate the spatial migration of the EASM margin since the LGM. Correspondingly, there is an estimated 350-km migration distance between the LGM and the mid-Holocene, and a minimum 150-km northwestward migration of the monsoon rain belt during the warm Holocene, compared with the present day (**Figure 4**). Similarly, using an *M. angigyra* abundance of 2.5% as a reference, we estimate a northwesterly monsoon rain belt advance of ~300 km for the warm Holocene compared with the cold LGM, and a ~100-km northwestward migration compared with the present day (**Figure 5**). We estimate that the distributions of mollusk species shifted to the northwestern sites at average rates of ~30 km/ka during ~15–12 ka (from the onset of the deglacial warming) and ~50 km/ka during ~12–9 ka (roughly corresponding to the early Holocene).

DISCUSSION

Precipitation and related humidity conditions are important first-order factors affecting mollusk communities at large regional scale, especially on the northern margin of the EASM in northern China (Chen and Gao, 1987; Wu et al., 2018; Dong et al., 2019). Previous studies have shown that the two mollusk species are highly sensitive to monsoonal precipitation, which is supported by our surveys of modern mollusk abundance, and their abundance in Chinese loess deposits has been widely used to reconstruct changes in EASM intensity during the Quaternary (Wu et al., 2002; Wu et al., 2018). Our records show that the abundance of these mollusks increased substantially with climatic warming during the last deglaciation, reaching a maximum during ~8–4 ka. The maximum timing of EASM intensity indicated by the mollusk records during the mid-Holocene is consistent with that documented by climatically-sensitive records of magnetic susceptibility, organic matter content and carbon isotopes from Chinese loess deposits (Lu et al., 2013). It is also supported by pollen-based precipitation reconstructions from lake deposits in northern China (Chen et al., 2015; Zhou et al., 2016; Wen et al., 2017; Cheng et al., 2020), indicating that the maximum summer monsoon precipitation on the northern EASM margin occurred in the mid-Holocene, rather than during the early Holocene, as inferred from speleothem oxygen isotope records.

The northern margin of the EASM rain belt, as inferred from the two mollusk indicator species, shifted from northwest to southeast, consistent with records of loess grain-size and C_4 plant biomass records (Yang and Ding, 2008; Yang et al., 2015). Previous studies have presented only two time slices and did not demonstrate a statistical linkage between spatial shifts of the rain belt and climatic warming. We found that observed spatial shifts were significantly greater during intervals of high-amplitude warming. Specifically, a pronounced extension of the EASM rain belt occurred at ~16 ka, corresponding to the beginning of the last deglaciation. The estimated maximum advance rate reached ~50 km/ka during ~12–9 ka, corresponding to the interval of rapid warming from the last deglaciation to the Holocene. These results indicate that the rate and extent of EASM rainfall expansion were strongly related to the concurrent level of warming since the last deglaciation.

It is noteworthy that the ecological requirements of the two EASM indicator mollusk species are not the same. The distribution of the maximum abundance and extension of the two species differ slightly due mainly to the different optimum ranges of hydrothermal conditions. *M. angigyra* requires warmer and wetter conditions for its survival and growth and tends to be located in the south with higher precipitation. As shown in our fossil record, their fossils are only distributed at a few sites in the southeastern Loess Plateau, such as at Weinan during the cold LGM (Wu et al., 2002). The most obvious expansion (characterized by continuous occurrence and 3–5% abundance isolines) of *M. angigyra* has been from the southern CLP to the central CLP since deglaciation, while *P. orphana* can extend northwestward from the central CLP to the northwest. Thus, the extension rate and amplitude of the EASM rain belt indicative of their reference abundance value may deviate slightly, but the path and direction of their expansion still coincide with the modern precipitation pattern. Both two mollusks indicate a roughly 300-km northwestward migration of the monsoon rain belt for the warm Holocene compared with the cold LGM. Although our reconstruction would be improved by a higher temporal resolution, better chronological accuracy, and more fossil sites, our data provide the best estimates of extension rates and is an improvement over previous study.

Our estimated migration distance is similar to that of the desert margin from the LGM to the mid-Holocene inferred from loess grain-size records (Yang and Ding, 2008). This estimate is also consistent with the 300-km northwestward migration of the monsoon rain belt inferred from the spatial distribution of C_4 plant biomass in the CLP (Yang et al., 2015). Although the migration distance estimated by different proxies may vary due to proxy sensitivity and the accuracy of the chronology, the same northwestward trend provides firm evidence of the extension of the EASM rain belt based on both ecological and geochemical proxies.

Our data, together with previous geological records, confirm that increased global temperatures strengthened the EASM and resulted in at least 150 km concomitant northward advance of the monsoon rain belt during the mid-Holocene compared to today. This long-term linkage between climatic warming and monsoon rainfall extent is supported by recent climate models, namely the coincidence of the increased land-ocean thermal contrast with the Asian monsoon domain, which was forced mainly by Earth orbital parameters and atmospheric CO_2 content, since the last deglaciation (Cheng et al., 2020). This evidence supports the scenario proposed by Broecker and Putnam (2013) that the Northern Hemisphere warms more rapidly than the Southern Hemisphere oceans. This leads to an increase in the interhemispheric temperature contrast which induces a northward shift of the thermal equator (ITCZ), ultimately leading to increased precipitation on the northern margin of monsoonal Asia. These scenarios occurred during earlier warm periods, such as the mid-Pliocene (Huang et al., 2019). As a result, northern China may become wetter over the next century as global warming continues. We, therefore, suggest that the drying trend in northern China, which has already lasted for several decades, will eventually reverse with ongoing global warming.

CONCLUSION

Based on 356 surface-soil mollusk assemblages we demonstrate that two dominant mollusk species, *Punctum orphana* and *Macrochlamys angigyra*, can be used as an indicator of the movement of the EASM rain belt. Based on this, we present changes in the abundance of the two species from six loess sections across the Chinese Loess Plateau, and examine spatiotemporal changes in the EASM rain belt during the interval from the cold LGM to the warm Holocene. The spatial distribution of the abundances of the two mollusk species shows a northeast-southwest zonal distribution for both the present-day, the cold LGM, and the warm mid-Holocene, which is consistent with the northeast-southwest trend of modern precipitation. Therefore, the northeast-southwest zonal distribution pattern of mollusk abundance in the CLP is a robust analog for the EASM rain belt. The occurrence of the two EASM indicator species shows a lag from the relatively warm, wet southeast to the relatively cold, dry northwest since the LGM, with their abundance reaching a maximum during the mid-Holocene. Using the 3–5% mollusk abundance isolines as a reference, we estimate that the EASM rain belt during the warm Holocene penetrated 150-km further northwestward compared to today. Our results provide long-term biological evidence suggesting that the northern monsoonal marginal region in China may become wetter as the climate warms, and thus that the observed drought trend of recent decades may be reversed with ongoing global warming.

DATA AVAILABILITY STATEMENT

The original contributions presented in the study are included in the article/**Supplementary Material**, further inquiries can be directed to the corresponding authors.

AUTHOR CONTRIBUTIONS

YD conceived the study, undertook the field work, collected the mollusk data, identified and counted the mollusk species, performed statistical analyses, and wrote the text. NW conceived the study, undertook the field work, collected the mollusk data, and wrote the text; FL undertook the field work, collected the mollusk data, and wrote the text. HL conceived the study, undertook the field work, collected the mollusk data, and wrote the text. All authors commented on the interpretation of the results and gave final approval for publication.

FUNDING

This work was supported by the "Strategic Priority Research Program" of the Chinese Academy of Sciences (XDB26000000) and the National Natural Science Foundation of China (41888101, 42172210, 41830322, and 41430103).

ACKNOWLEDGMENTS

We thank Drs Linpei Huang, Bin Wu, Daojing Wang, and Wenwen Wen for their assistance with the fieldwork.

SUPPLEMENTARY MATERIAL

The Supplementary Material for this article can be found online at: https://www.frontiersin.org/articles/10.3389/feart.2021.788738/full#supplementary-material

REFERENCES

Broecker, W. S., and Putnam, A. E. (2013). Hydrologic Impacts of Past Shifts of Earth's thermal Equator Offer Insight into Those to Be Produced by Fossil Fuel CO_2. *Proc. Natl. Acad. Sci.* 110, 16710–16715. doi:10.1073/pnas.1301855110

Chase, T. N., Knaff, J. A., Pielke, R. A., and Kalnay, E. (2003). Changes in Global Monsoon Circulations since 1950. *Nat. Hazards* 29, 229–254. doi:10.1023/A:1023638030885

Chen, D. N., and Gao, J. X. (1987). *Economic Fauna Sinica of China, Terrestrial Mollusca*. Beijing: Science Press.

Chen, F., Xu, Q., Chen, J., Birks, H. J. B., Liu, J., Zhang, S., et al. (2015). East Asian Summer Monsoon Precipitation Variability since the Last Deglaciation. *Sci. Rep.* 5, 11186. doi:10.1038/srep11186

Cheng, H., Edwards, R. L., Broecker, W. S., Denton, G. H., Kong, X., Wang, Y., et al. (2009). Ice Age Terminations. *Science* 326, 248–252. doi:10.1126/science.1177840

Cheng, H., Edwards, R. L., Wang, Y., Kong, X., Ming, Y., Kelly, M. J., et al. (2006). A Penultimate Glacial Monsoon Record from Hulu Cave and Two-phase Glacial Terminations. *Geology* 34, 217–220. doi:10.1130/G22289.1

Cheng, J., Ma, Y., Wu, H., Long, H., and Liu, Z. (2020). Migration of Afro-Asian Monsoon Fringe since Last Glacial Maximum. *Front. Earth Sci.* 8, 322. doi:10.3389/feart.2020.00322

Cheng, Y., Liu, H., Dong, Z., Duan, K., Wang, H., and Han, Y. (2020). East Asian Summer Monsoon and Topography Co-determine the Holocene Migration of forest-steppe Ecotone in Northern china. *Glob. Planet. Change* 187, 103135. doi:10.1016/j.gloplacha.2020.103135

Ding, Y. (2004). "Seasonal March of the East-Asian Summer Monsoon," in *East Asian Monsoon*. Editor C. P. Chang (Singapore: World Scientific Publishing Co. Pte. Ltd), 3–53. doi:10.1142/9789812701411_0001

Ding, Y., Wang, Z., and Sun, Y. (2008). Inter-decadal Variation of the Summer Precipitation in East China and its Association with Decreasing Asian Summer monsoon.Part I: Observed Evidences. *Int. J. Climatol.* 28, 1139–1161. doi:10.1002/joc.1615

Dong, Y., Wu, N., Jiang, W., Li, F., and Lu, H. (2020b). Cascading Response of flora and Terrestrial Mollusks to Last Deglacial Warming. *Glob. Ecol. Conserv.* 24, e01360. doi:10.1016/j.gecco.2020.e01360

Dong, Y., Wu, N., Li, F., Chen, X., Zhang, D., Zhang, Y., et al. (2019). Influence of Monsoonal Water-Energy Dynamics on Terrestrial Mollusk Species-Diversity Gradients in Northern China. *Sci. Total Environ.* 676, 206–214. doi:10.1016/j.scitotenv.2019.04.292

Dong, Y., Wu, N., Li, F., Huang, L., Lu, H., and Stenseth, N. C. (2021b). Paleorecords Reveal the Increased Temporal Instability of Species Diversity under Biodiversity Loss. *Quat. Sci. Rev.* 269, 107147. doi:10.1016/j.quascirev.2021.107147

Dong, Y., Wu, N., Li, F., Huang, L., and Wen, W. (2015). Time-transgressive Nature of the Magnetic Susceptibility Record across the Chinese Loess Plateau at the Pleistocene/Holocene Transition. *PLoS One* 10, e0133541. doi:10.1371/journal.pone.0133541

Dong, Y., Wu, N., Li, F., and Lu, H. (2021a). Coupled Morphologic and Demographic Responses of *Opeas Striatissimum* (Gastropoda: Subulinidae) to Latest Pleistocene to Early Holocene Climate Fluctuations. *Palaeogeogr. Palaeoclimatol. Palaeoecol.* 562, 110101. doi:10.1016/j.palaeo.2020.110101

Dong, Y., Wu, N., Li, F., Zhang, D., Zhang, Y., Huang, L., et al. (2020a). Anthropogenic Modification of Soil Communities in Northern China for at Least Two Millennia: Evidence from a Quantitative Mollusk Approach. *Quat. Sci. Rev.* 248, 106579. doi:10.1016/j.quascirev.2020.106579

Draxler, R. R., and Hess, G. D. (1997). "Description of the HYSPLIT_4 Modeling System," in *NOAA Tech. Memo. ERL ARL-224* (Silver Spring: Air Resources Laboratory), 24. Available at: https://www.researchgate.net/publication/255682850_Description_of_the_HYSPLIT_4_modelling_system.

Goldsmith, Y., Broecker, W. S., Xu, H., Polissar, P. J., deMenocal, P. B., Porat, N., et al. (2017). Northward Extent of East Asian Monsoon Covaries with Intensity on Orbital and Millennial Timescales. *Proc. Natl. Acad. Sci. USA* 114, 1817–1821. doi:10.1073/pnas.1616708114

Held, I. M., and Soden, B. J. (2006). Robust Responses of the Hydrological Cycle to Global Warming. *J. Clim.* 19, 5686–5699. doi:10.1175/JCLI3990.1

Horsák, M., Juřičková, L., Horsáková, V., Pokorná, A., Pokorný, P., Šizling, A. L., et al. (2018). Forest Snail Diversity and its Environmental Predictors along a Sharp Climatic Gradient in Southern Siberia. *Acta Oecol.* 88, 1–8. doi:10.1016/j.actao.2018.02.009

Huang, X., Jiang, D., Dong, X., Yang, S., Su, B., Li, X., et al. (2019). Northwestward Migration of the Northern Edge of the East Asian Summer Monsoon during the Mid-pliocene Warm Period: Simulations and Reconstructions. *J. Geophys. Res. Atmos.* 124, 1392–1404. doi:10.1029/2018JD028995

Huber, C., Leuenberger, M., Spahni, R., Flückiger, J., Schwander, J., Stocker, T. F., et al. (2006). Isotope Calibrated Greenland Temperature Record over Marine Isotope Stage 3 and its Relation to CH4. *Earth Planet. Sci. Lett.* 243, 504–519. doi:10.1016/j.epsl.2006.01.002

Isaaks, E. H., and Srivastava, R. M. (1989). *An Introduction to Applied Geostatistics*. New York: Oxford University Press.

Lai, Z.-P., and Wintle, A. G. (2006). Locating the Boundary between the Pleistocene and the Holocene in Chinese Loess Using Luminescence. *The Holocene* 16, 893–899. doi:10.1191/0959683606hol980rr

Li, F. J., Wu, N. Q., Dong, Y. J., Lu, H. Y., Chen, X. Y., Zhang, D., et al. (2016). Quantitative Distribution and Calculation of Ecological Amplitude of Land Snail Metodontia in the Chinese Loess Plateau and Adjacent Regions. *Quat. Sci.* 36, 564–574. (In Chinese with English abstract). doi:10.11928/j.issn.1001-7410.2016.03.06

Li, F., Wu, N., and Rousseau, D.-D. (2006). Preliminary Study of Mollusk Fossils in the Qinan Miocene Loess-Soil Sequence in Western Chinese Loess Plateau. *Sci. China Ser. D* 49, 724–730. doi:10.1007/s11430-006-0724-7

Li, J., Wu, Z., Jiang, Z., and He, J. (2010). Can Global Warming Strengthen the East Asian Summer Monsoon? *J. Clim.* 23, 6696–6705. doi:10.1175/2010JCLI3434.1

Lin, Z. H., Mo, X. G., Li, H. X., and Li, H. B. (2002). Comparison of Three Spatial Interpolation Methods for Climate Variables in China. *Acta Geograph. Sin.* 57, 47–56. doi:10.11821/xb200201006

Liu, J., Chen, J., Zhang, X., Li, Y., Rao, Z., and Chen, F. (2015). Holocene East Asian Summer Monsoon Records in Northern China and Their Inconsistency with Chinese Stalagmite $\delta^{18}O$ Records. *Earth-Science Rev.* 148, 194–208. doi:10.1016/j.earscirev.2015.06.004

Liu, T. S. (1985). *Loess and the Environment*. Haidian: China Ocean Press.

Lu, H., Wu, N., Liu, K., Jiang, H., and Liu, T. (2007). Phytoliths as Quantitative Indicators for the Reconstruction of Past Environmental Conditions in China II: Palaeoenvironmental Reconstruction in the Loess Plateau. *Quat. Sci. Rev.* 26, 759–772. doi:10.1016/j.quascirev.2006.10.006

Lu, H., Yi, S., Liu, Z., Mason, J. A., Jiang, D., Cheng, J., et al. (2013). Variation of East Asian Monsoon Precipitation during the Past 21 k.Y. And Potential CO_2 Forcing. *Geology* 41, 1023–1026. doi:10.1130/G34488.1

Maher, B. A., and Thompson, R. (2012). Oxygen Isotopes from Chinese Caves: Records Not of Monsoon Rainfall but of Circulation Regime. *J. Quat. Sci.* 27, 615–624. doi:10.1002/jqs.2553

Nekola, J. C. (2003). Large-scale Terrestrial Gastropod Community Composition Patterns in the Great Lakes Region of North America. *Divers. Distrib.* 9, 55–71. doi:10.1046/j.1472-4642.2003.00165.x

Peterse, F., Prins, M. A., Beets, C. J., Troelstra, S. R., Zheng, H., Gu, Z., et al. (2011). Decoupled Warming and Monsoon Precipitation in East Asia over the Last Deglaciation. *Earth Planet. Sci. Lett.* 301 (1–2), 256–264. doi:10.1016/j.epsl.2010.11.010

Qian, L. Q. (1991). *Climate of the Loess Plateau*. Beijing: China Meteorological Press.

Richter, C., Roettig, C.-B., Wolf, D., Groh, K., Kolb, T., and Faust, D. (2019). Changes in Pleistocene Gastropod Faunas on Fuerteventura (Canary Islands) and Implications on Shifting Palaeoenvironmental Conditions. *Quat. Sci. Rev.* 209, 63–81. doi:10.1016/j.quascirev.2019.02.005

Rousseau, D.-D., and Wu, N. (1997). A New Molluscan Record of the Monsoon Variability over the Past 130 000 Yr in the Luochuan Loess Sequence, China. *Geology* 25, 275–278. doi:10.1130/0091-613(1997)025<0275:ANMROT>2.3

Rousseau, D.-D., Wu, N., Pei, Y., and Li, F. (2009). Three Exceptionally strong East-Asian Summer Monsoon Events during Glacial Times in the Past 470 Kyr. *Clim. Past* 5, 157–169. doi:10.5194/cpd-4-1289-200810.5194/cp-5-157-2009

Rousseau, D.-D., Wu, N. Q., and Guo, Z. T. (2000). The Terrestrial Mollusks as New Indices of the Asian Paleomonsoons in the Chinese Loess Plateau. *Glob. Planet. Change* 26, 199–206. doi:10.1016/S0921-8181(00)00086-2

Shakun, J. D., Clark, P. U., He, F., Marcott, S. A., Mix, A. C., Liu, Z., et al. (2012). Global Warming Preceded by Increasing Carbon Dioxide Concentrations during the Last Deglaciation. *Nature* 484, 49–54. doi:10.1038/nature10915

Sibson, R. (1981). "A Brief Description of Natural Neighbor Interpolation," in *Interpolation Multivariate Data* (New York: John Wiley & Sons), 21–36.

Sümegi, P., Náfrádi, K., Molnár, D., and Sávai, S. (2015). Results of Paleoecological Studies in the Loess Region of Szeged-Öthalom (SE Hungary). *Quat. Int.* 372, 66–78. doi:10.1016/j.quaint.2014.09.003

Tan, M. (2009). Circulation Effect: Climatic Significance of the Short-Term Variability of the Oxygen Isotopes in Stalagmites from Monsoonal China: Dialogue between Paleoclimate Records and Modern Climate Research. *Quatern. Sci.* 29, 851–862. (In English abstract). doi:10.3969/j.issn.1001-7410.2009.05.01

Wang, H. (2001). The Weakening of the Asian Monsoon Circulation after the End of 1970's. *Adv. Atmos. Sci.* 18, 376–386. doi:10.1007/BF02919316

Wang, S., Gong, D., and Zhu, J. (2001a). Twentieth-century Climatic Warming in China in the Context of the Holocene. *The Holocene* 11, 313–321. doi:10.1191/095968301673172698

Wang, Y. J., Cheng, H., Edwards, R. L., An, Z. S., Wu, J. Y., Shen, C.-C., et al. (2001b). A High-Resolution Absolute-Dated Late Pleistocene Monsoon Record from Hulu Cave, China. *Science* 294, 2345–2348. doi:10.1126/science.1064618

Webster, P. J., Magaña, V. O., Palmer, T. N., Shukla, J., Tomas, R. A., Yanai, M., et al. (1998). Monsoons: Processes, Predictability, and the Prospects for Prediction. *J. Geophys. Res.* 103, 14451–14510. doi:10.1029/97JC02719

Webster, R., and Oliver, M. A. (2001). *Geostatistics for Environmental Science*. Toronto: John Wiley & Sons.

Wen, R., Xiao, J., Fan, J., Zhang, S., and Yamagata, H. (2017). Pollen Evidence for a Mid-Holocene East Asian Summer Monsoon Maximum in Northern China. *Quat. Sci. Rev.* 176, 29–35. doi:10.1016/j.quascirev.2017.10.008

Wu, N., Chen, X., Rousseau, D., Li, F., Pei, Y., and Wu, B. (2007). Climatic Conditions Recorded by Terrestrial Mollusc Assemblages in the Chinese Loess Plateau during marine Oxygen Isotope Stages 12-10. *Quat. Sci. Rev.* 26, 1884–1896. doi:10.1016/j.quascirev.2007.04.006

Wu, N., Li, F., and Rousseau, D.-D. (2018). Terrestrial Mollusk Records from Chinese Loess Sequences and Changes in the East Asian Monsoonal Environment. *J. Asian Earth Sci.* 155, 35–48. doi:10.1016/j.jseaes.2017.11.003

Wu, N., Liu, T., Liu, X., and Gu, Z. (2002). Mollusk Record of Millennial Climate Variability in the Loess Plateau during the Last Glacial Maximum. *Boreas* 31, 20–27. doi:10.1111/j.1502-3885.2002.tb01052.x

Wu, N. Q., Rousseau, D. D., and Liu, T. S. (1996). Land Mollusk Records from the Luochuan Loess Sequence and Their Paleoenvironmental Significance. *Sci. China, Ser. D Earth Sci.* 39, 494–502.

Wu, N., Rousseau, D. D., and Liu, D. (1999). Climatic Instability Recorded by the Mollusk Assemblages from the Late Glacial Loess Deposits in China. *Chin.Sci.Bull.* 44, 1238–1242. doi:10.1007/bf02885974

Wu, N., Rousseau, D. D., Liu, T., Lu, H., Zhaoyan, G., Guo, Z., et al. (2001). Orbital Forcing of Terrestrial Mollusks and Climatic Changes from the Loess Plateau of China during the Past 350 Ka. *J. Geophys. Res.* 106, 20045–20054. doi:10.1029/2001JD900224

Wu, N., Rousseau, D. D., and Liu, X. (2000). Response of Mollusk Assemblages from the Luochuan Loess Section to Orbital Forcing since the Last 250 Ka. *Chin.Sci.Bull.* 45, 1617–1622. doi:10.1007/bf02886225

Yang, S., and Ding, Z. (2008). Advance-retreat History of the East-Asian Summer Monsoon Rainfall belt over Northern China during the Last Two Glacial-Interglacial Cycles. *Earth Planet. Sci. Lett.* 274, 499–510. doi:10.1016/j.epsl.2008.08.001

Yang, S., Ding, Z., Li, Y., Wang, X., Jiang, W., and Huang, X. (2015). Warming-induced Northwestward Migration of the East Asian Monsoon Rain belt from the Last Glacial Maximum to the Mid-holocene. *Proc. Natl. Acad. Sci. U.S.A.* 112, 13178–13183. doi:10.1073/pnas.1504688112

Yen, T. C. (1939). Die Chinesischen land-und Süsswasser Gastropoden des naturmuseums senckenberg. *Abhandlumgen der Senckenbergischen Naturforschenden Gesellschaft* 444, 1–235.

Zhou, X., Sun, L., Zhan, T., Huang, W., Zhou, X., Hao, Q., et al. (2016). Time-transgressive Onset of the Holocene Optimum in the East Asian Monsoon Region. *Earth Planet. Sci. Lett.* 456, 39–46. doi:10.1016/j.epsl.2016.09.052

Conflict of Interest: The authors declare that the research was conducted in the absence of any commercial or financial relationships that could be construed as a potential conflict of interest.